Nature (London) 227, 271.
Kuntz, I. D., Jr., Brassfield, T. S., Law, G. D., and Purcell, G. V. (1969), *Science 163*, 1329.
Kupke, D. W. (1966), *Fed. Proc., Fed. Amer. Soc. Exp. Biol. 25*, 990.
Kupke, D. W., Hodgins, M. G., and Beams, J. W. (1972), *Proc. Nat. Acad. Sci. U. S. 69*, 2258.
Leonard, B. R., Anderegg, J. W., Shulman, S., Kaesberg, P., and Beeman, W. W. (1953), *Biochim. Biophys. Acta 12*, 499.
Lin, S. H. C., Dewan, R. K., Bloomfield, V. A., and Morr, C. V. (1971), *Biochemistry 10*, 4788.
Lipkin, M. R., Davison, J. A., Harvey, W. T., and Kurtz, S. S. (1944), *Ind. Eng. Chem. 16*, 55.
Marvin, D. A., and Hoffmann-Berling, H. (1963), *Z. Naturforsch. 18B*, 884.
Möller, W. J. (1964), *Proc. Nat. Acad. Sci. U. S. 51*, 501.
Overby, L. R., Barlow, G. H., Doi, R. H., Jacob, M., and Spiegelman, S. (1966), *J. Bacteriol. 91*, 442.
Pecora, R. (1964), *J. Chem. Phys. 40*, 1604.
Pusey, P. N., Koppel, D. E., Schaefer, D. W., Camerini-Otero, R. D., and Franklin, R. M. (1972), *J. Phys. Paris 33*, C1-163.
Pusey, P. N., Koppel, D. E., Schaefer, D. W., Camerini-Otero, R. D., and Koenig, S. H. (1974), *Biochemistry 13*, 952.
Putnam, F. W. (1954), *J. Polym. Sci. 12*, 391.
Reisler, E., and Eisenberg, H. (1969), *Biochemistry 8*, 4572.
Salditt, M., Braunstein, S. N., Camerini-Otero, R. D., and Franklin, R. M. (1972), *Virology 48*, 259.
Scatchard, G. (1946), *J. Amer. Chem. Soc. 68*, 2315.
Silbert, J. A., Salditt, M., and Franklin, R. M. (1969), *Virology 39*, 666.
Sinha, N. K., Fujimura, R. K., and Kaesberg, P. (1965), *J. Mol. Biol. 11*, 84.
Steitz, J. A. (1968), *J. Mol. Biol. 33*, 937.
Strauss, E. G., and Kaesberg, P. (1970), *Virology 42*, 437.
Strauss, J. H., and Sinsheimer, R. L. (1963), *J. Mol. Biol. 7*, 43.
Svedberg, T., and Pedersen, K. O. (1940), The Ultracentrifuge, London, Oxford University Press.
Tanford, C. (1961), Physical Chemistry of Macromolecules, New York, N. Y., Wiley.
Vasquez, C., Granboulan, N., and Franklin, R. M. (1966), *J. Bacteriol. 92*, 1779.
Weber, K., Rosenbusch, J., and Harrison, S. C. (1970), *Virology 41*, 763.
Yamamoto, K. R., Alberts, B. M., Benzinger, R., Lawhorne, L., and Treiber, G. (1970), *Virology 40*, 734.
Zipper, P., Kratky, O., Herrmann, R., and Hohn, T. (1971), *Eur. J. Biochem. 18*, 1.

Conformation of Retinal Isomers†

R. Rowan, III,‡ A. Warshel,§ B. D. Sykes,*,¶ and M. Karplus

ABSTRACT: The solution conformations of the polyene chain portions of *all-trans*-retinal and 11-*cis*-retinal have been investigated by ^{1}H nuclear magnetic resonance (nmr) spectroscopy, including measurements of long-range nuclear spin coupling constants, chemical shifts, spin–lattice relaxation times, and nuclear Overhauser enhancements. Theoretical calculations of the minimum energy conformations and torsional potentials of these molecules are also presented. The results show that the polyene chain of *all-trans*-retinal has a planar conformation in solution with all of the single bonds from 7-C to 15-C in the s-trans conformation. The polyene chain of 11-*cis*-retinal is shown to be essentially planar in the regions 7-C to 10-C and 13-C to 15-C, but is twisted slightly from planarity around the 10–11 single bond and exists as an equilibrium between two low-energy conformers, distorted s-cis and distorted s-trans, about the 12–13 single bond. In acetone at low temperature the distorted s-trans conformation appears to be preferred.

The conjugated polyene aldehyde 11-*cis*-retinal is the chromophore of the visual pigment. It is isomerized to the 11-trans compound in the photochemical reaction of vision. Subsequent dark reactions, involving both the chromophore and the protein opsin to which it is attached through an imine linkage, result ultimately in a nervous impulse and the sensation of vision (Wald, 1968). The solution conformation of the retinal isomers (see Figure 1) is therefore of considerable interest for an understanding of the nature of the visual pigment. Two features of the conformation of the retinal isomers require particular attention: the orientation of the β-ionone ring relative to the polyene chain and the conformation of the polyene chain itself, especially with respect to the stereochemistry about the 10–11 and 12–13 single bonds in the 11-cis isomer. The torsional angle of the β-ionone ring in *all-trans*-[1] and 11-*cis*-retinal has been determined in the crystal by X-ray analysis (Hamanaka *et al.*, 1972; Gilardi *et al.*, 1972), measured in solution by use of nuclear magnetic resonance (nmr) spectroscopy (Honig *et al.*, 1971), and calculated theo-

† From the Department of Chemistry, Harvard University, Cambridge, Massachusetts 02138. *Received July 23, 1973.* Supported in part by grants from the National Science Foundation (GP-36104X) and from the National Institutes of Health (EY-00062, GM-17190, and RR-000292 (NMR Facility for Biomedical Studies)).

‡ National Science Foundation Predoctoral Fellow, 1968–1972. Present address: Department of Chemistry, Carnegie-Mellon University, Pittsburgh, Pa. 15213.

§ Present address: Department of Chemical Physics, Weizmann Institute, Rehovot, Israel.

¶ Alfred P. Sloan Fellow, 1971–1973.

[1] The term "*all-trans*" is used in accord with the current convention for this isomer, which is predominantly distorted s-cis with respect to the 6–7 bond (Figure 1) (Honig *et al.*, 1971).

retically (Honig *et al.*, 1971; Pullman *et al.*, 1969; Langlet *et al.*, 1970). In the present study the conformation of the polyene chain portion of *all-trans*- and 11-*cis*-retinal is examined by nmr and semiempirical quantum-mechanical calculations. Earlier experimental investigations include the important nmr studies of Patel (1969) and Patel and Shulman (1970) and the recent crystal-structure determinations of *all-trans*- (Hamanaka *et al.*, 1972) and 11-*cis*-retinal (Gilardi *et al.*, 1972); published theoretical work concerned with establishing the minimum energy conformation includes that of Nash (1969) and of Honig and Karplus (1971).

Methods

In this section, we outline the experimental and theoretical methods used for investigating the structure of 11-*cis*- and *all-trans*-retinal.

Experimental. Three types of ^1H nmr measurements were used to obtain information about the solution conformation of *all-trans*- and 11-*cis*-retinal: (1) proton spin–spin coupling constants, (2) nuclear Overhauser enhancements (NOE's), and (3) nuclear spin–lattice relaxation times (T_1's). Nmr measurements at 100 MHz were made on Varian HA-100 and XL-100-15 nmr spectrometers, both of which were interfaced with Varian 620i computers for Fourier transform operation and conventional time averaging. The ambient probe temperature of both spectrometers was 32 ± 1°; the probe temperature was calibrated in the usual manner with methanol. Double resonance measurements on the HA-100 were facilitated by the use of a voltage divider box in combination with a Wavetek Model 114 voltage controlled oscillator. This allowed the frequency of the irradiating radiofrequency field to be switched between a resonance position, which could be easily and accurately adjusted, and preset off-resonance positions. The accuracy of the conventional time averaging was improved by using a simple variable-gain, variable-offset amplifier to amplify the spectrometer output so that the signal made full use of the dynamic range (±10 V) of the analog to digital converter. Nmr (250 MHz) spectra were obtained on the MPC-HF 250 superconducting spectrometer operating at 25° (Dadok *et al.*, 1970). The samples were prepared in deuterioacetone at approximately 0.5 M concentration with a small amount of hexamethyldisiloxane (1–2%, v/v) as an internal standard. All samples were carefully degassed by several freeze–pump–thaw cycles and then sealed. *all-trans*-Retinal was purchased from Eastman and used without further purification. The 11-*cis*-retinal was a generous gift from Paul K. Brown.

Coupling constants and chemical shifts were obtained by computer fitting of carefully time-averaged spectra; as many as 30 spectra were accumulated to allow the complete assignment of weak lines. The iterative program LAOCOON3 (Bothner-By and Castellano, 1964) and the noniterative spectrum computing and plotting program SIMEQ (C. W. Kort and P. J. Van der Haak, private communication) were used to compare calculated and observed spectra. All resonance frequencies obtained from 9-CH_3 and 13-CH_3 decoupled spectra and used for iterative fitting were corrected for Bloch-Siegert shifts of the reference (lock) signal (Johnson, 1965).

NOE's were determined by a comparison of the relative areas of the observed peak with the irradiating radiofrequency field H_2 first on resonance ("irradiated spectrum") and then far-off resonance ("control spectrum") for the saturated nucleus. The H_2 field strength was kept at approximately 1 mG for the irradiation of methyl resonances, and up to 2.5 mG for the irradiation of 10-H.[2] The power used to irradiate the methyl resonances was sufficient to maximize $f_{15\text{-H}}$(13-CH_3) without affecting neighboring methyl resonances.[3] The power used to irradiate 10-H at 250 MHz was probably insufficient to completely saturate all of the lines of the 10-H multiplet. NOE's at 250 MHz were determined by alternately collecting two to four irradiated and control spectra. Peak areas were then measured by planimetry (three to ten times for each peak), and a fractional enhancement was calculated from the average irradiated and control areas as follows: $f_d(s)$ = (average irradiated area − average control area)/average control area. All of the enhancements at 100 MHz were obtained with the aid of either continuous wave (CW) or Fourier transform (FT) time averaging. Control and irradiated spectra were collected alternately (from 3 to 25 of each) and stored on magnetic tape. Peak areas were determined by planimetry as above, or by digital integration. In this manner enhancements could be measured for extremely weak lines. The Fourier transform NOE experiments were performed using pulse delays between transients greater than or equal to five times the T_1 of the observed spin during double irradiation (Noggle and Shirmer, 1971; S. L. Patt and R. Rowan, unpublished results), and both with the decoupler on or off during the acquisition of the free induction decay. The observed FT NOE's were equal to the CW NOE's. Each enhancement listed is the average of several complete determinations.

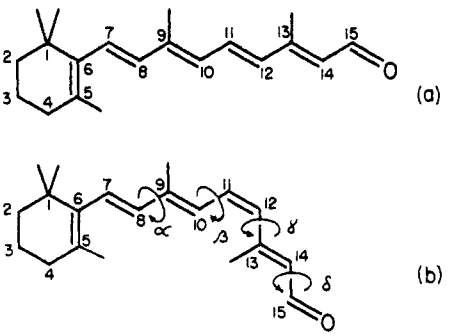

FIGURE 1: Isomers of retinal: (a) *all-trans*-retinal; (b) 11-*cis*-retinal. The sense of dihedral angles ($\alpha,\beta,\gamma,\delta$) is determined by looking along a C–C single bond of interest from the lower numbered carbon to the higher numbered carbon. A clockwise rotation of the higher numbered carbon then corresponds to the positive torsional angle. The completely s-trans conformer (for both isomers) corresponds to a value of 180° for all of the torsional angles.

Predicted enhancements were obtained for various possible values of the torsional angles with bond lengths and bond angles set equal to the following values: olefinic C–H bond length, 1.08 Å, and methyl C–H bond length, 1.09 Å (Sutton, 1965); aldehyde C–H bond length, 1.11 Å (Traetteberg, 1970); polyene C–C bond lengths, from reported structures of *all-trans*- and 11-*cis*-retinal (Hamanaka *et al.*, 1972; Gilardi *et al.*, 1971, 1972); and C–C–C bond angle, 120°. The methyl protons were assumed to be located at the center of the H–H–H triangle (see below).

Nmr spin–lattice relaxation times were determined at 100 MHz using the partially relaxed Fourier transform method (Vold *et al.*, 1968). The 180° pulse length on the XL-100 spectrometer was 52 μsec.

[2] H_2 field strength calibrated from Bloch-Siegert shifts (Johnson, 1965).

[3] Notation: $f_d(s)$ = fractional enhancement of spin d when spin s is saturated.

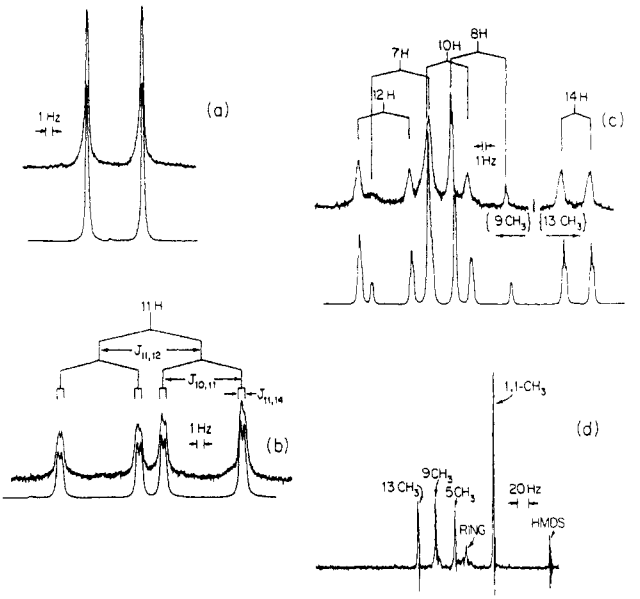

FIGURE 2: Observed and simulated 100-MHz nmr spectra of *all-trans*-retinal. A seven-spin system (7-H, 8-H, 10-H, 11-H, 12-H, 14-H, 15-H) was used in the simulation, with the chemical shifts and coupling constants from Tables I and II: (a) spectrum of 15-H, with 13-CH_3 decoupled; (b) spectrum of 11-H with 9-CH_3 decoupled; (c) spectrum of 7-H, 8-H, 10-H, 12-H region, with 9-CH_3 decoupled, and of 14-H, with 13-CH_3 decoupled (neglected in this calculated spectrum is the coupling of 7-H to 5-CH_3 and 4,4′-H (Honig *et al.*, 1971); and (d) spectrum of the methyl and methylene protons of the ring.

Theoretical. To determine the ground-state equilibrium geometry and potential surface, a semiempirical technique was used (Warshel and Karplus, 1972). It is based on the approximation of σ–π separability; the σ-electron energy is given by a set of empirical potential functions and the π-electron energy is evaluated by an SCF–LCAO–MO method of the Pariser–Parr–Pople type corrected for nearest neighbor overlap. All the parameters determining the π-electron integrals and the σ-electron potential functions have been obtained by a simultaneous refinement procedure based on fitting ground- and excited-state energies, conformations, and vibrational frequencies of a series of conjugated molecules. The present method, in contrast to earlier simplified semiempirical procedures (Nash, 1969; Honig and Karplus, 1971), is designed to permit variation of all aspects of the molecular geometry (*i.e.*, bond lengths, bond angles, and torsional angles). In this way, the effect of steric interactions on bond lengths and bond angles, as well as on torsional angles, can be taken into account in finding the minimum energy geometry and the potential surface of the molecule.

TABLE I: Coupling Constants for Retinal Isomers.

	All-Trans		11-Cis	
H_i,H_j	$J_{i,j}$ (Hz)	How Determined	$J_{i,j}$ (Hz)	How Determined
7,8	16.2	Observed[a]	16.2	Observed[a]
7,10	0.55	Homologous to 11,14[b]	0.55	Line shape of 10[d]
8,10	−0.6	Observed[a]	−0.55	Observed[a]
8,11	0.1	Homologous to 12,15[b]	0.1	Line shape of 8[d]
8,12	−0.05	Simulation[c]	−0.05	Simulation[c]
10,11	11.5	Observed[a]	12.41	Observed[a]
10,12	−0.6	Homologous to 8,10[b]	−0.85	Observed[a]
10,14	−0.05	Simulation[c]	−0.15	Sharpening[e]
11,12	15.0	Observed[a]	12.13[f]	Observed[a]
11,14	0.55	Observed[a]	0.4	Observed[a]
12,14	−0.6	Homologous to 8,10[b]	0.95	Observed[a]
12,15	0.15	Line shape of 15[d]	0.2	Line shape of 12,15[d]
14,15	7.94	Observed[a]	7.87	Observed[a]
7,9	0.15	Sharpening[e]	0.15	Sharpening[e]
8,9	0.15	Sharpening[e]	0.1	Sharpening[e]
9,10	1.25	Observed[a]	1.1	Observed[a]
9,11	0.1	Sharpening[e]	0.0	
9,12	0.1	Sharpening[e]	0.25	Sharpening[e]
9,14	0.0		0.15	Sharpening[e]
10,13	0.1	Sharpening[e]	0.05	Sharpening[e]
11,13	0.1	Sharpening[e]	0.15	Sharpening[e]
12,13	0.1	Sharpening[e]	0.1	Sharpening[e]
13,14	1.25	Observed[a]	1.25	Observed[a]
13,15	0.25	Observed[a]	0.18	Observed[a]

[a] Observed, observed as splitting in the spectrum. [b] Homologous, assumed to exist because of the observation of a similar coupling (*i.e.*, over a similar configuration of bonds) and required for a better simulation of the line shape in the final spectrum. [c] Simulation, small but markedly improve the final simulated spectrum by removing extraneous small peaks. [d] Line shape, added to improve the simulation of the line shape after all other contributions to the line width including nuclear spin relaxation and magnetic field inhomogeneities have been considered. [e] Sharpening, observed as a sharpening of the resonance during decoupling indicating the presence of an unresolved coupling; magnitude estimated by simulation of both coupled and decoupled spectra. [f] $J_{11\text{-H},12\text{-H}}$ observed at 12.13 Hz at 32° and 11.83 Hz at 25°.

Results

Experimental. The nmr results are divided into three parts: coupling constants and chemical shifts, NOE's, and T_1's. We consider first the coupling constants and chemical shifts. The 100-MHz nmr spectrum of *all-trans*-retinal is shown in Figure 2. The coupling constants obtained for *all-trans*-retinal from both 100- and 250-MHz spectra are listed in Table I and the chemical shifts are listed in Table II. The long-range coupling constants were obtained in several ways. Some of the splittings due to long-range coupling were directly observable in the spectrum. For example, $J_{9\text{-}CH_3,10\text{-H}}$ and $J_{13\text{-}CH_3,14\text{-H}}$ were observed as splittings of 9-CH_3 and 13-CH_3, respectively; $J_{8\text{-H},10\text{-H}}$ was observed as a splitting of 8-H; and $J_{11\text{-H},14\text{-H}}$ was observed as a splitting of 11-H. The last was verified by the collapse of the doublet character of each line of the 11-H quartet upon the irradiation of 14-H. Some splittings were observed as a sharpening of resonance lines during double irradiation. For example, $J_{8\text{-H},9\text{-}CH_3}$ could be observed as a sharpening of 8-H upon the irradiation of 9-CH_3. Thirdly, some couplings were assumed to exist because of the observation of a similar coupling (*i.e.*, over a similar configuration of bonds) in another part of the molecule. For example, $J_{10\text{-H},12\text{-H}}$ and $J_{12\text{-H},14\text{-H}}$ are homologous with $J_{8\text{-H},10\text{-H}}$, and $J_{7\text{-H},10\text{-H}}$ is homologous with $J_{11\text{-H},14\text{-H}}$. Finally, some

TABLE II: Chemical Shifts of Retinal Isomers.

Resonance	All-Trans[a]	11-Cis[a]
1,1′-CH_3	0.974 (−0.015)	0.962 (−0.005)
2,2′-H	1.41	1.40
3,3′-H	1.55	1.54
4,4′-H	1.95	1.95
5-CH_3	1.649 (+0.010)	1.630 (+0.017)
9-CH_3	1.986 (+0.020)	1.935 (+0.039)
13-CH_3	2.294 (+0.036)	2.322 (+0.095)
7-H	6.319 (−0.019)	6.308 (+0.014)
8-H	6.144 (+0.015)	6.150 (+0.076)
10-H	6.206 (+0.047)	6.584 (+0.139)
11-H	7.226 (+0.079)	6.676 (+0.117)
12-H	6.399 (+0.077)	5.965 (+0.094)
14-H	5.838 (+0.035)	5.876 (+0.016)
15-H	10.049 (+0.043)	10.017 (+0.060)

[a] Parts per million relative to hexamethyldisiloxane at 32°; values in parentheses are the change in chemical shift in going to low temperatures (−47° for all-trans and −52° for 11-cis).

couplings were introduced because certain resonances appeared broader than expected from the known magnetic field inhomogeneities and nuclear spin relaxation times, indicating a splitting pattern too complex to be resolvable. The tabulated values for all of the coupling constants and chemical shifts were obtained by comparing calculated and observed spectra. All of the nonzero couplings included in the list made significant differences in the calculated spectrum. Coupling constants listed as negative in Table I indicate that the simulation was appreciably better with this choice of relative sign. The best calculated spectra are not perfect, however, because of our inability due to limited computer memory size to simulate the spectrum of the total spin system of the molecule including methyl and ring protons.

The corresponding coupling constants and chemical shifts obtained in the same manner for 11-*cis*-retinal are listed in Tables I and II, respectively. The most significant differences in the long-range coupling constants are $J_{10\text{-H},12\text{-H}}$ and $J_{12\text{-H},14\text{-H}}$. The latter is observed as a splitting of the upfield half of the 14-H doublet (from coupling to 15-H) in the 13-CH_3 irradiated spectrum. In the undecoupled spectrum, the upfield half of the 14-H doublet is approximately a 1:4:6:4:1 five-line pattern from about equal coupling to 12-H and 13-CH_3. $J_{10\text{-H},12\text{-H}}$ is observed in the spectrum as a more complex pattern for the downfield half of the 12-H doublet (from coupling to 11-H) than would be expected on the basis of coupling to only 14-H. The final coupling constants and chemical shifts for 11-*cis*-retinal were obtained by computer fitting of the spectrum. The observed and calculated 100-MHz spectra are shown in Figure 3. These spectra and the 250-MHz spectra (Figure 4a) were best simulated with $J_{10\text{-H},12\text{-H}} = -0.85$ Hz and $J_{12\text{-H},14\text{-H}} = \pm 0.95$ Hz. The calculated spectra were sensitive to the sign of $J_{10\text{-H},12\text{-H}}$ relative to $J_{10\text{-H},11\text{-H}}$ and $J_{11\text{-H},12\text{-H}}$ taken as positive. Once a reasonable set of line assignments had been made, LAOCOON3 invariably iterated to a negative value for $J_{10\text{-H},12\text{-H}}$, regardless of the initial guess at its sign. However, LAOCOON3 (five-spin fit only: 10-H, 11-H, 12-H, 14-H, 15-H) tended to make the coupling constant $J_{10\text{-H},12\text{-H}}$ more negative ($J_{10\text{-H},12\text{-H}} = -1.65$ Hz). It is only when comparisons were made with the program SIMEQ, in which 9-CH_3 was included, that the correct magnitude for

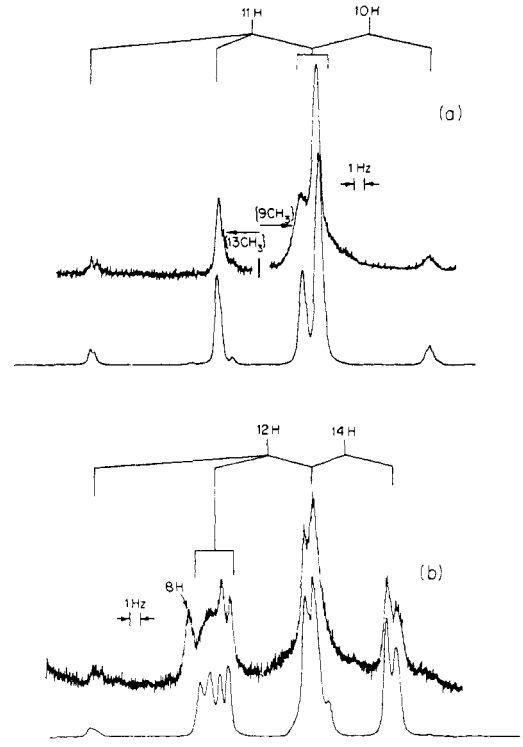

FIGURE 3: Observed and simulated 100-MHz nmr spectra of 11-*cis*-retinal. (a) Top trace, 10-H–11-H region of observed nmr spectrum; the downfield peaks of 11-H multiplet, with 13-CH_3 decoupled; the upfield peaks, with 9-CH_3 decoupled. Bottom trace, simultated spectrum for a seven-spin system (7-H, 8-H, 10-H, 11-H, 12-H, 14-H, 15-H) using chemical shifts and coupling constants from Tables I and II. (b) Top trace, observed 12-H–14-H region, with 13-CH_3 decoupled; also including upfield peak of 8-H doublet. Bottom trace, simulated spectrum for X_3ABCDE system (9-CH_3, 10-H, 11-H, 12-H 14-H, 15-H) using chemical shifts and coupling constants from Tables I and II.

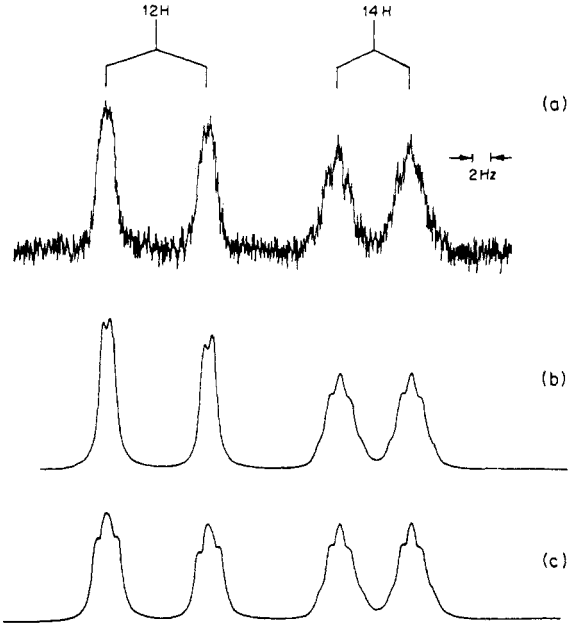

FIGURE 4: Observed and simulated 250-MHz nmr spectra of 11-*cis*-retinal: (a) observed 12-H–14-H region, with 9-CH_3 decoupled; (b) simulated spectrum for X_3ABCDE system (13-CH_3, 10-H, 11-H, 12-H, 14-H, 15-H) using coupling constants and chemical shifts from Tables I and II, except with $J_{11\text{-H},12\text{-H}} = 11.83$ Hz; (c) simulated spectrum with $J_{10\text{-H},12\text{-H}} = +0.85$ Hz.

TABLE III: Nuclear Overhauser Enhancements of Retinal Isomers.[a]

		Obsd							
	Irr	7	8	10	11	12	14	15	
all-trans-Retinal at 100 MHz, 32°	9-CH_3	18	4	0	17	0	0	0	All ±2
	13-CH_3	0	0	0	18	0	0	31	
	14-H							3	
all-trans-Retinal at 100 MHz, −47°	9-CH_3			0	15	0	0	0	All ±2
	13-CH_3				18	0	0	30	
all-trans-Retinal at 250 MHz, 25°	9-CH_3	18	5	−1		0			All ±2
	13-CH_3	1	−1	0		−1			
11-*cis*-Retinal at 100 MHz, 32°	9-CH_3	13	5	0	23	0	0	0	All ±2 except as noted
	10-H						12		
	13-CH_3	0	0	11	2	0	1	30	
	14-H							6 ± 3	
11-*cis*-Retinal at 100 MHz, −47°	9-CH_3	12	4	0	20	0	0	0	All ±2
	10-H						7	0	
	13-CH_3	0	0	11	0	0	0	31	
11-*cis*-Retinal at 250 MHz, 25°	9-CH_3	16	7	3	22	−3	1		All ±3
	10-H						>5		
	13-CH_3	−1	0	12	0	5	−4	33	

[a] Enhancements are in per cent.

$J_{10\text{-H},12\text{-H}}$ was obtained. The sensitivity of the calculated spectra to the relative sign of $J_{10\text{-H},12\text{-H}}$ is further demonstrated by the simulation of the 250-MHz spectra (Figure 4b,c). The simulated spectra were not sensitive to the relative sign of $J_{12\text{-H},14\text{-H}}$.

The NOE's measured for the chain portion of *all-trans*- and 11-*cis*-retinal at 100 and 250 MHz are listed in Table III. Where resonances overlapped in the 100-MHz spectra, the enhancements were determined as follows: for *all-trans-retinal*, $f_{10\text{-H}}(s)$ from the upfield half of the 10-H doublet after correction for $f_{8\text{-H}}(s)$, $f_{12\text{-H}}(s)$ from the downfield half of the 12-H doublet after correction for $f_{7\text{-H}}(s)$; for 11-*cis*-retinal, $f_{10\text{-H}}(s)$ from the upfield resonance of the 10-H multiplet, $f_{11\text{-H}}(s)$ from the downfield resonances of the 11-H multiplet, $f_{12\text{-H}}(s)$ from the downfield half of the 12-H doublet after correction for $f_{8\text{-H}}(s)$.

TABLE IV: Spin–Lattice Relaxation Times of Retinal Isomers at 100 MHz.

	All-Trans			11-Cis	
		Calcd[b]			Calcd[b]
Resonance	Obsd[a]	*c*	*d*	Obsd[a]	*e*
HMDS	9.9			10.5	
1,1′-CH_3	1.0			1.2	
Ring	1.1			1.3	
5-CH_3	2.1			2.4	
9-CH_3	1.9			2.4	
13-CH_3	2.1			3.0	
7-H				2.6	
8-H	1.9			2.6	
10-H	1.4	1.4	1.4	2.2	2.2
11-H	1.7	0.7	1.4	2.0	1.3
12-H	1.7	1.3	1.4	3.2	2.8
14-H	2.9	2.4	2.1	6.0	5.3
15-H	5.7	1.3	2.6	8.2	2.0

[a] T_1's in seconds, all standard deviations $\lesssim 5\%$, except 10-H of 11-cis which is 10%. [b] Normalized to 10-H. [c] Assuming planar conformation, 120° C–C–C and C–C–H bond angles. [d] Calculated using bond angles from X-ray structure (Hamanaka *et al.*, 1972). [e] Assuming conformation $\beta = 165°$, $\gamma = 90°$.

The spin–lattice relaxation times measured for *all-trans*- and 11-*cis*-retinal at 100 MHz are listed in Table IV. Where resonances overlapped, T_1's were determined for the same resonances that are listed above for the NOE measurements.

Theoretical. The theoretical calculations were used to determine the ground-state geometry of *all-trans*- and 11-*cis*-retinal. Table V gives the results obtained and compares them with the available X-ray data. Detailed crystal structures have now been reported for both *all-trans*-retinal (Hamanaka *et al.*, 1972) and 11-*cis*-retinal (Gilardi *et al.*, 1972).

Discussion

We consider first the theoretical results and their correspondence with the crystal structures for *all-trans*- and 11-*cis*-retinal. We then describe the use of coupling constants, NOE's, and T_1's for determining the conformations of the chain portions of *all-trans*- and 11-*cis*-retinal in solution. The conformations with respect to the 8–9, 10–11, 12–13, and 14–15 single bonds can be described in terms of the torsional angles α, β, γ, and δ, respectively (Figure 1). The convention used is the standard one for torsional angles; *i.e.*, the direction of rotation shown corresponds to positive angles, and the planar s-cis conformation is taken as 0° (Klyne and Prelog, 1960).

Theoretical. From Table V, the agreement between the calculated and experimental values is satisfactory in that most of the important structural features are reproduced. However, it is clear from Table V that there are quantitative differences which reflect, in part, the inaccuracies in the semi-empirical technique used for the geometry calculations, al-

TABLE V: Calculated and Observed (Crystal) Structures.

A. *all-trans*-Retinal						B. 11-*cis*,12*s*-*cis*-Retinal					
θ[a]	Calcd	Obsd[b]	*b* (Å)[c]	Calcd	Obsd[b]	θ[a]	Calcd	Obsd[g]	*b*[c]	Calcd	Obsd[g]
1,2,3	110.9	(115.8)[d]	6,1	1.497	1.535	1,2,3	110.9	111.5	6,1	1.497	1.528
2,3,4	108.8	(115.6)[d]	1,2	1.537	(1.545)[d]	2,3,4	108.8	111.9	1,2	1.537	1.523
3,4,5	112.3	(115.2)[d]	2,3	1.528	(1.420)[d]	3,4,5	112.3	113.3	2,3	1.528	1.498
4,5,6	123.9	122.6	3,4	1.527	(1.494)[d]	4,5,6	123.9	122.9	3,4	1.526	1.532
5,6,7	121.5	122.2	4,5	1.500	1.505	5,6,7	121.8	123.2	5,6	1.361	1.333
6,5,5′[e]	123.1	124.3	5,6	1.358	1.330	6,5,5′[e]	123.3	125.8	6,7	1.491	1.486
6,7,8	123.2	124.3	6,7	1.495	1.482	6,7,8	123.8	126.2	7,8	1.353	1.339
7,8,9	123.4	126.3	7,8	1.351	1.315	7,8,9	124.3	126.4	8,9	1.479	1.461
8,9,10	117.8	118.2	8,9	1.479	1.467	8,9,10	117.6	117.8	9,10	1.364	1.347
9,10,11	125.8	127.1	9,10	1.365	1.345	9,10,11	125.4	125.3	10,11	1.463	1.454
9′,9,10[e]	123.1	123.4	10,11	1.464	1.442	9′,9,10[e]	123.0	124.3	11,12	1.361	1.339
10,11,12	120.5	123.4	11,12	1.361	1.338	10,11,12	126.0	128.1	12,13	1.468	1.472
11,12,13	125.5	125.6	12,13	1.467	1.452	11,12,13	128.6	129.9	13,14	1.375	1.358
12,13,14	117.9	118.2	13,14	1.375	1.344	12,13,14	122.6	121.3	14,15	1.429	1.467
13,14,15	124.0	125.9	14,15	1.428	1.455	13,14,15	123.6	122.9	15,16	1.22	1.213
ϕ[f]						ϕ[f]					
6,1,2,3	−46	(−42.6)[d]				6,1,2,3	−46	−47.4			
1,2,3,4	63	(50.0)[d]				1,2,3,4	62	59.1			
2,3,4,5	−48	(−31.8)[d]				2,3,4,5	−49	−39.8			
3,4,5,6	18	(6.8)[d]				3,4,5,6	18	11.5			
4,5,6,7	179	178.6				4,5,6,7	178	180.4			
5,6,7,8	−50	−58.3				5,6,7,8	−44	−41.4			
6,7,8,9	183	180.7				6,7,8,9	182	179.6			
7,8,9,10	168	175.8				7,8,9,10	173	174			
8,9,10,11	182	179.1				8,9,10,11	178	175.5			
9,10,11,12	173	180.1				9,10,11,12	170	179.3			
10,11,12,13	182	175.5				10,11,12,13	−9	−2.1			
11,12,13,14	172	181.6				11,12,13,14	−29	−38.7			
12,13,14,15	180	177.7				12,13,14,15	180	179.8			

[a] Bond angles in degrees. [b] Hamanaka *et al.*, 1972. [c] Bond lengths in ångströms. [d] Uncertain due to thermal motion and/or disorder. [e] Primed atom is methyl carbon. [f] Torsional angles in degrees. [g] Gilardi *et al.*, 1972.

though errors in the structure determination and crystal interactions may also contribute. To indicate some of the differences we look at Table VA for *all-trans*-retinal. It should be noted that the experimental results involving atoms 2 and 3 of the cyclohexene ring are not reliable because of disorder in the crystal; *i.e.*, the presence of two different "half-chair" conformations leads to an average structure with a projected 2-C–3-C bond length that is too short and projected angles (*e.g.*, (2,3,4)) that are too large. For the bond angles θ, the calculated and X-ray values are generally within ±1° with most of the deviations from the "standard" angle of 120° given correctly by the calculations. However, there are somewhat larger disagreements for the angles (7,8,9) and, particularly, (10,11,12). The calculated and measured bond lengths are mostly within ±0.02 Å of each other, but again there are a number of larger deviations and the relative values among nominal single and double bonds are not always correctly reproduced by the calculations; *e.g.*, the (6,1) and (7,8) bonds show a large disagreement and the (14,15) bond, which is calculated to be one of the shortest "single" bonds, is found to be one of the longest. Comparing with 11-*cis*-retinal, we see that a corresponding disagreement exists for the (14,15) bond in this molecule, but that the (6,1) and (7,8) bonds are closer to the calculated value. Since the (14,15) bond length depends significantly on the oxygen parameters, which were not as carefully optimized in model compounds as those for carbon and hydrogen, it is likely that the calculations are in error. For the (6,1) and (7,8) bonds the situation is less clear, the measurement of 1.315 Å for the conjugated 7,8 double bond being a surprisingly short value. Turning to the torsional angles ϕ in *all-trans*-retinal, we see that the larger deviations from planarity are rather well reproduced by the calculations, but that for the essentially planar trans configurations, the theoretical and experimental results show little correlation. If anything, for the part of the chain from 8-C to 15-C there is an inverse correlation (in terms of which torsional angles are larger or smaller than 180°), suggesting that the calculations found a nearly planar geometry that is a relative minimum different from the one present in the crystal.

The geometries of *all-trans*- and 11-*cis*-retinal are seen to be similar except for the region involving carbons 10–14. Also, there is a small, but interesting, difference between the β-ionone ring orientations of the two molecules, the calculated and X-ray structures both having the ring torsional angle (6-C–7-C) significantly larger in *all-trans*- than in 11-*cis*-retinal. This is correlated with the difference in bond order P_{67} for the 6-C–7-C bond in the two molecules (P_{67} equals 0.243 in all-trans and 0.260 in 11-cis).

In the 10-C–14-C region, as indicated above, the all-trans results (Table VA) show that the conjugated chain is essen-

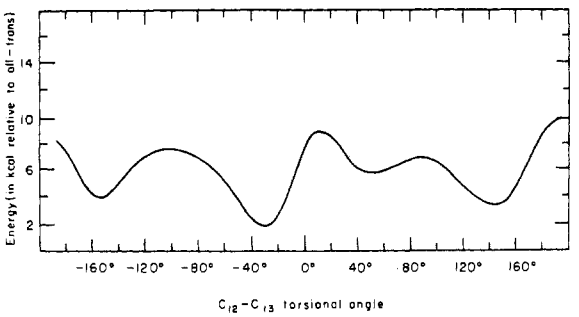

FIGURE 5: Calculated "adiabatic" potential for twisting around 12-C–13-C single bond (see text).

tially planar with calculated deviations of ±3° and bond lengths and bond angles corresponding to those found in the remainder of the chain. By contrast, the 11-cis molecule is significantly altered in the 10-C–14-C region. Although the bond lengths are only slightly different from their values in all-trans (±0.02 Å), the bond angles and torsional angles are very different. It is seen that all of the C–C–C bond angles (10,11,12; 11,12,13; and 12,13,14) are larger (up to ~6°) in 11-*cis*- than *all-trans*-retinal so as to minimize the steric repulsion. As to the torsional angles, the X-ray results and the calculations agree that the dominant deviation from planarity is about the 12-C–13-C bond; the calculations also suggest some twisting about 10-C–11-C (~10°) and about 11-C–12-C (~9°), but the measured values for the crystal show no such distortion (1° for 10-C–11-C and 2° for 11-C–12-C).

Since the observed X-ray structure may be affected by the presence of intermolecular forces in the crystal, it is important to have independent data for the conformation in the solution. This is of particular interest in the present case because of the form of the calculated potential function for twisting about the various bonds in the 11-cis molecule. As found in earlier work (Honig and Karplus, 1971) and confirmed here, the steric hindrance between the hydrogen on 10-C and the remainder of the conjugated chain can be relieved by twisting the molecule about the 12-C–13-C bond into either a distorted 12-s-cis or 12-s-trans conformation. To illustrate this point, we show in Figure 5 the calculated "adiabatic" potential for twisting around the 12-C–13-C bond. This curve is obtained by locally minimizing the energy of the molecule for each value of the 12-C–13-C angle. The lack of symmetry in the potential (*e.g.*, about 0 and 180°) results from the fact that the 12-C–13-C rotation was carried out sequentially in both directions from the absolute minimum at −29° and that for each angle the remainder of the molecule is distorted adiabatically. Thus, there is a completely equivalent surface obtained by reflecting the illustrated curve through 0°. It is of interest to compare the present results with those obtained earlier with a simplified theoretical model (Honig and Karplus, 1971). There the calculated barriers at 0 and 180° are much higher than in the present treatment, primarily because no relaxation of the bond angles was permitted in the earlier study.

From Figure 5 and an evaluation of its reliability, it is clear that in themselves the calculations cannot with certainty demonstrate that for the 11-cis molecule in solution only one conformation relative to 12-C–13-C contributes significantly; that is, there are at least two low-energy structures (distorted s-cis, $\gamma = -30°$; distorted s-trans, $\gamma = 150°$) that have a calculated energy difference of only 1.5 kcal/mol. Thus, it is very important to determine experimentally whether one or both structures are present in solution, even though the crystal structure corresponds to 12-s-cis.

Coupling Constants and Chemical Shifts. Comparison of the observed proton–proton coupling constants in the polyene chain of *all-trans*- and 11-*cis*-retinal shows that although many of them are the same, certain important couplings are different. In what follows the coupling constants listed in Table I that are expected to be sensitive to the conformation of the polyene chain are discussed and an attempt is made to draw conclusions from them concerning the geometries of the two isomers. The points we make supplement the work of Patel (1969), whose paper has already provided an analysis for the use of vicinal couplings for this purpose. All of the coupling constants involving hydrogens or methyl groups bonded to carbons 7–10 and to carbons 13–15 are seen to be effectively identical for *all-trans*- and 11-*cis*-retinal. Furthermore, their values are in agreement with an essentially planar, all-trans conformation for these parts of the molecule. In particular, the long-range $J_{8\text{-H},10\text{-H}}$, $J_{8\text{-H},9\text{-CH}_3}$, and $J_{15\text{-H},13\text{-CH}_3}$ couplings are expected on theoretical grounds to be sensitive to deviations from planarity (Karplus, 1960, 1969). For $J_{8\text{-H},10\text{-H}}$ which is of the allylic type, the value −0.6 Hz is close to that obtained for the corresponding coupling in *s-trans*-butadiene (−0.83 Hz, Hobgood and Goldstein, 1964; Cooper *et al.*, 1970), −0.80 Hz (Segre and Castellano, 1972). The "isopropylidenic" $J_{8\text{-H},9\text{-CH}_3}$ coupling is very small (0.1–0.15 Hz), in accord with expectations if 8-H is in the plane of the 9-C–10-C double bond (Barfield and Chakrabarti, 1969; Holmes and Kivelson, 1961). For $J_{15\text{-H},13\text{-CH}_3}$, the coupling is of the homoallylic type and has the small value (~0.1–0.2 Hz) expected for an essentially planar geometry (Karplus, 1960, 1969; Barfield and Chakrabarti, 1969). The vicinal $J_{14\text{-H},15\text{-H}}$ coupling of 7.9 Hz in both molecules is, as pointed out by Patel (1969), in agreement with the measured value for acrolein (Douglas and Goldstein, 1965); its small magnitude relative to the trans coupling in a molecule like ethane appears to be a consequence in part of the electronegative oxygen substituent and in part of the larger H–C–C′ bond angles (*e.g.*, compare with the $J_{10\text{-H},11\text{-H}}$ value of 11.5 Hz and the trans coupling of 18 Hz in ethane).

Turning to the coupling constants between pairs of protons in the set 9-H–14-H, we find a number of important correspondences and differences between *all-trans*- and 11-*cis*-retinal. For the vicinal $J_{11\text{-H},12\text{-H}}$ coupling, the difference is simply that expected between a trans and a cis ethylenic linkage (Karplus, 1959). The difference between $J_{7\text{-H},8\text{-H}}$ and $J_{11\text{-H},12\text{-H}}$ probably reflects the slightly lower bond order and greater bond length of the latter (*i.e.*, $P_{7,8} = 0.92$ and $P_{11,12} = 0.88$). As to $J_{10\text{-H},11\text{-H}}$, it is of interest that the coupling is slightly larger in 11-cis than all-trans; any deviation from planarity in the former would be expected to reduce the value since the vicinal coupling is very sensitive to the dihedral angle. One possible explanation of the larger value in 11-cis is that the conformational calculations have shown that the 11-H–11-C–10-C angle is smaller in 11-cis than in all-trans as a result of the steric repulsion that leads to opening of the 10-C–11-C–12-C angle (~120° in all-trans, 126° in 11-cis). Calculations of the H–C–C′ angular dependence of the vicinal coupling yield a change of the right order of magnitude. There are also possible contributions from the change in the π-bond order and bond lengths of 10-C–11-C (Langlet and Giessner-Prettre, 1972). Further confirmation for the essential planarity about the 10–11 bond is provided by the long-range $J_{11\text{-H},9\text{-CH}_3}$ and the $J_{10\text{-H},12\text{-H}}$ couplings, which are of the homoallylic and allylic type, respectively. The $J_{11\text{-H},9\text{-CH}_3}$ coupling is very small in both 11-*cis*- and *all-trans*-retinal

and equal to the $J_{7\text{-H},9\text{-CH}_3}$ value. Since a strong angular dependence has been demonstrated experimentally and theoretically for this coupling, the near-zero value is significant (Karplus, 1960, 1969; Barfield and Chakrabarti, 1969). For 10-H and 12-H, the all-trans and 11-cis results are slightly different, with the former (−0.6 Hz) slightly smaller in magnitude than the latter (−0.85 Hz). This appears not to arise directly from the fact that all-trans has a cisoid arrangement of the coupled hydrogens while they are transoid in 11-cis, since for butadiene the two types of couplings are the same (−0.85 Hz). There could be a change in the σ contributions to the two couplings due to the C–C–C angle difference mentioned above, but this has not been examined theoretically. Also, there is the possibility that the difference between all-trans and 11-cis implies some twisting of the 10-C–11-C bond in the latter.

Of considerable interest is the $J_{12\text{-H},14\text{-H}}$ coupling, whose value is −0.6 Hz in all-trans and (±)0.95 Hz in 11-cis. These results are to be compared with the $J_{10\text{-H},12\text{-H}}$ values for the two compounds (−0.6 Hz in all-trans, −0.85 Hz in 11-cis) and the butadiene coupling, which corresponds to planar all-trans, of −0.85 Hz. There is no good model compound for the planar 11-cis,12-s-cis conformation, while the planar 11-cis,12-s-trans would correspond to the same butadiene coupling of −0.85 Hz. Because of the significant values of both σ and π type contributions for this type of four-bond coupling, the theoretical results are not unequivocal. The most extensive calculations are those of Barfield for the related, though not entirely equivalent, propene-like system (Barfield, 1971). Comparison of the work of Bothner-By and Jung for hindered butadienes (1968) with that of Barfield on transoid couplings suggests that a similar angular dependence is expected. The INDO calculations of Barfield yield negative values of the cisoid coupling corresponding to $J_{12\text{-H},14\text{-H}}$ for all dihedral angles around the 12-C–13-C nominal single bond. Further, the values become increasingly negative as the system deviates from planarity whether from the s-cis ($\phi = 0$) or the s-trans ($\phi = 180°$) conformation. It is of interest that the calculated values for the range in the neighborhood of s-cis are smaller in magnitude than those around s-trans, so that for the former an out-of-plane angle of approximately 30° would be required to obtain the experimental coupling of 0.95 Hz. However, the quantitative understanding of the variation of these couplings is too uncertain to draw a definite conclusion concerning the angle.

It is worth mentioning that the values of other couplings, which we have not discussed in detail (*e.g.*, $J_{8\text{-H},11\text{-H}}$ and $J_{12\text{-H},15\text{-H}}$ of the homoallylic type), are consistent with the conclusions described above, though larger out-of-plane angles than seem possible would be required to obtain significant changes in their values. Correspondingly, other couplings (*e.g.*, $J_{10\text{-H},9\text{-CH}_3}$ and $J_{14\text{-H},13\text{-CH}_3}$) have values consistent with the theoretical results for them. Finally, there are many very small long-range couplings (*e.g.*, $J_{10\text{-H},14\text{-H}}$) which appear reasonable, but would require more detailed calculations for their interpretations.

In summary, the observed coupling constants for *all-trans*-retinal specify an essentially planar geometry, while those for 11-*cis*- indicate essential planarity except for the 12-C–13-C and possibly the 10-C–11-C bond. As to the question of whether the 12-C–13-C bond is s-cis or s-trans in solution, it is not resolved by the coupling constant results and their analysis.

An analysis of the chemical shifts in the different retinal isomers was given by Patel (1969). Our results are in agreement with his with the exception that 12-H and 14-H are interchanged in acetone-d_6. The largest chemical shift changes between *all-trans*- and 11-*cis*-retinal are for 10-H (+0.378 ppm), 11-H (−0.450 ppm), and 12-H (−0.434 ppm), all of which experience significantly different environments in the two isomers. A simple model for the chemical shifts based upon localized bond anisotropy contributions (ApSimon *et al.*, 1967a,b, 1970) was unsuccessful in explaining the observed chemical-shift differences. Without suitable model compounds and an adequate theoretical framework for the interpretation of their chemical shifts, the chemical shifts cannot be used at this point to provide quantitative information about the conformation of the 11-cis isomer.

Nuclear Overhauser Effect and Relaxation Times. NOE's and spin–lattice relaxation times can be interpreted in terms of relative internuclear distances. An expression relating the fractional enhancement, $f_d(s)$

$$f_d(s) = \frac{1}{2}\left(\frac{r_{ds}^{-6}}{R_d}\right) - \frac{1}{2}\sum_{n\neq d,s}\left(\frac{r_{dn}^{-6}}{R_d}\right)f_n(s) \qquad (1)$$

of the detected spin d when the spin s is saturated has been derived by Noggle and Schirmer (Schirmer *et al.*, 1970) under the assumptions that (1) the relaxation is dominated by intramolecular dipole–dipole interactions, (2) the saturated nuclei are at most loosely coupled to the observed nuclei, and (3) the relaxation of all of the spins can be characterized by a single correlation time. In eq 1, r_{ds} is the distance between the spins d and s, and $R_d = \Sigma_i r_{di}^{-6}$. Using this expression, with the additional assumption that the methyl group protons can be represented by three protons at the center of the equilateral triangle described by their internuclear vectors, a set of fractional enhancements and relative spin–lattice relaxation times ($1/T_1 \propto R_d$) can be predicted as a function of the possible torsional angles.

The observed NOE's at 100 and 250 MHz[4] for *all-trans*-retinal show that the only large enhancements are $f_{7\text{-H}}(9\text{-CH}_3)$, $f_{11\text{-H}}(9\text{-CH}_3)$, $f_{11\text{-H}}(13\text{-CH}_3)$, and $f_{15\text{-H}}(13\text{-CH}_3)$; that is, 15-H is relaxed almost entirely by 13-CH_3, 11-H is relaxed equally by 9-CH_3 and 13-CH_3, and 7-H is relaxed by 9-CH_3 with some contribution from the ring methyl groups. Given that the polyene chain of *all-trans*-retinal is essentially planar in solution as demonstrated by the arguments presented in the previous sections, we use the comparison of the observed NOE's and T_1's with the NOE's and T_1's calculated for the planar conformation as a test of the assumptions involved in the model. The calculated NOE's and T_1's obtained from eq 1 and the structural parameters given under Methods are listed in Tables VI and IV, respectively. In agreement with the observed results, the only calculated enhancements which are large are $f_{11\text{-H}}(9\text{-CH}_3)$, $f_{11\text{-H}}(13\text{-CH}_3)$, and $f_{15\text{-H}}(13\text{-CH}_3)$; we have not included $f_{7\text{-H}}(9\text{-CH}_3)$, which is also large, because the ring methyl protons which also relax 7-H (Honig *et al.*, 1971) were not included in the calculation. The calculated NOE's are all larger than the observed enhancements. This is in the direction expected if other relaxation mechanisms contribute to the relaxation of the observed nuclei (*i.e.*, $R_d = \Sigma_i r_{di}^{-6} + \rho_{other}$). One other relaxation mechanism is intramolecular dipole–dipole relaxation among the three protons of the CH_3 group. However, while this is an important relaxation pathway for the CH_3 protons themselves, its inclusion in the NOE calculation has only a very small effect (<1%) upon

[4] No significant differences were observed between the 100- and 250-MHz NOE's for well-resolved resonances (*i.e.*, $f_{15\text{-H}}(13\text{-CH}_3)$).

TABLE VI: Calculated Nuclear Overhauser Enhancements for *all-trans*-Retinal.[a]

	Irr	Observed 8-H	10-H	11-H	12-H	14-H	15-H
Exptl	9-CH_3	4	0	17	0	0	0
	13-CH_3	0	0	18	0	0	31
Calcd[b]	9-CH_3	7	2	24	−1	0	1
	13-CH_3	0	−1	22	2	3	45
Calcd[c]	9-CH_3	4	1	19	0	0	0
	13-CH_3	0	−1	23	2	1	42
Calcd[d]	9-CH_3	4	2	20	0	0	0
	13-CH_3	0	0	18	1	2	33

[a] Assuming planar structure. [b] Using 120° bond angles and including intramolecular dipole–dipole relaxation of methyl protons (see text). [c] Using bond angles from X-ray structure (Hamanaka *et al.*, 1972) and including intramolecular dipole–dipole relaxation of methyl protons (see text). [d] Using 120° bond angles and including intramolecular dipole–dipole relaxation of methyl protons and other relaxation pathways (ρ_{other}) for the C–H protons (see text).

the calculated NOE's for other protons. If one assumes arbitrarily that there is an additional relaxation mechanism (*e.g.*, intermolecular dipole–dipole interactions) which yields the same ρ_{other} contribution for all CH protons, calculated NOE's in close agreement with the observed NOE's can be obtained (Table VI); the magnitude of ρ_{other} required increases R_d for 11-H by 15–20%. Another effect is due to the difference between the true structure and the idealized 120° C–C–C bond angles used in the calculations. If the bond angles from the more open X-ray structure (see Table VA) are employed in obtaining the distances for eq 1, some of the calculated NOE's are closer to the observed NOE's (see Table VI). An additional factor contributing to the larger calculated NOE's may be that the distances used involving the methyl protons are too short (see T_1 discussion below).

The T_1 values, when normalized to 10-H, are also in good agreement with the observed values with the exception of 11-H and 15-H where the observed T_1's are longer than the calculated T_1's. For 10-H, 12-H, and 14-H, where the assumption of a single correlation time is most reasonable since their relaxation is dominated by neighboring chain protons (*e.g.*, 10-H by 8-H and 12-H; 12-H by 10-H and 14-H; etc.) and the CH_3 groups are not involved, the rotational correlation time τ_c calculated from dipole–dipole relaxation is 6×10^{-11} sec (assuming $\rho_{other} = 0$).[5] The fact that the calculated T_1's for 11-H and 15-H, whose relaxation is dominated by interactions with 9- and/or 13-CH_3, are too short suggests that either the effective correlation time for the H–CH_3 interaction is shorter than 6×10^{-11} sec or that the appropriate H–CH_3 distance to use in the NOE calculation is longer than the distance from the proton to the midpoint of the CH_3 triangle. ^{13}C nmr measurements indicate that internal rotation of 9-CH_3 and 13-CH_3 is more rapid than the rotational tumbling of the molecule as a whole; *i.e.* the ^{13}C T_1 for 13-CH_3 multiplied by the number of directly bonded protons is approximately 10 times longer than T_1 for 8-C, 10-C, 12-C, and 14-C (Kuhlman *et al.*, 1970; R. Rowan III, unpublished data). Under these conditions the H–CH_3 distance is more closely approximated by averaging $1/r^3$ for each proton of the methyl group over the internal rotation and then squaring this to obtain an effective $1/r^6$ (Wennerström, 1972; R. Rowan, J. A. McCammon, and B. D. Sykes, unpublished data). The result is that taking the H–CH_3 distance as the distance to the midpoint of the CH_3 group about compensates for the rapid internal rotation when the distances are averaged correctly, except for close distances where the appropriate distance can be longer than the distance to the CH_3 midpoint.

The calculated values of T_1 for 11-H and 15-H are lengthened (see Table IV) if the coordinates from the X-ray or the theoretical structure (see discussion of NOE's) are used. Also, if the 14–15 bond is twisted toward the s-cis conformation, T_1 for 15-H is further increased. While a 14–15 s-cis geometry is unlikely from coupling constant measurements and on the basis of "shift reagent" studies (Montaudo *et al.*, 1973; R. Rowan III, unpublished data), the ^{13}C T_1 for 15-C is significantly longer than for the other chain carbons, suggesting some torsional oscillations about the 14–15 single bond (R. Rowan III, unpublished data).

The possible conformations of 11-*cis*-retinal in solution were determined by comparing the observed NOE's with sets of calculated NOE's. For the calculation of enhancements, internuclear coordinates were computed for a series of possible conformations which were obtained by holding the torsional angles α and δ fixed at 180° and varying the torsional angles β and γ through a grid of values (β,γ) over the range $0° \leq \beta \leq 180°$, $0° \leq \gamma \leq 360°$ (note that $(\beta,\gamma) = (-\beta,-\gamma)$). All of the possible enhancements and the relative T_1's for each proton were then calculated for each conformation. The most informative results were those for which the calculated fractional enhancements varied markedly as a function of β and/or γ. The sensitive enhancements were $f_{11\text{-H}}$(9-CH_3), $f_{10\text{-H}}$(13-CH_3), $f_{12\text{-H}}$(13-CH_3), and $f_{14\text{-H}}$(10-H); a grid of the calculated values of these enhancements as a function of β and γ is shown in Table VII. A set of allowed values of the angles β and γ was then chosen using the criterion that the angle is "allowed" if the observed enhancement is less than the calculated enhancement for that choice of angle (see all-trans discussion and below). From the enhancements most sensitive to (β,γ) it is found that the only consistent set of allowed angles is ($\beta \simeq 165°$, $\gamma \simeq 90°$); the region ($\beta \simeq 165°$ to 180°, $\gamma \simeq -75°$ to $-90°$) is also almost satisfactory, though in this region no pair of angles is "allowed" for all of the enhancements. The other enhancements, which are less sensitive to (β,γ), also satisfy the criterion $NOE_{obsd} \leq NOE_{calcd}$ in these two regions. In addition the T_1's (within the limitations discussed for *all-trans*-retinal) agree reasonably well with the observed T_1's for either region (Table IV).

Although the above results show that for a single choice of (β,γ) it is possible to calculate the observed NOE's within the approximations of the model, it is important to note that the resulting (β,γ) values are in disagreement with those obtained from the other methods described above; that is, from (1) either of the structures (distorted s-cis and s-trans) corresponding to the two minima of the theoretical potential, (2) the structure suggested on the basis of the observed coupling constants, or (3) the X-ray structure. The essential difference between the NOE structure and all of the others is the large

[5] In general, even the definition of a single relaxation time for each nucleus in multispin systems is unjustified (Freeman *et al.*, 1970). However, the relaxation after the application of a nonselective π pulse to the whole spin system can be approximated theroetically and is observed experimentally to be characterized by a single exponential.

TABLE VII: Calculated Nuclear Overhauser Enhancements $f_{11\text{-H}}(9\text{-CH}_3)$, $f_{10\text{-H}}(13\text{-CH}_3)$, $f_{12\text{-H}}(13\text{-CH}_3)$, and $f_{14\text{-H}}(10\text{-H})$ for 11-*cis*-Retinal as a Function of the Torsional Angles β and γ.[a]

	γ =							
β	−135	−90	−45	0	45	90	135	180
				$f_{11\text{-H}}(9\text{-CH}_3)$				
180	32	32	32	32	32	32	32	32
135	24	24	24	23	24	24	24	23
90	10	10	9	10	10	10	10	10
45	3	2	2	3	3	3	2	3
				$f_{10\text{-H}}(13\text{-CH}_3)$				
180	41	13	1	0	1	13	41	49
135	41	15	2	0	0	5	24	45
90	25	7	2	0	0	1	8	26
45	8	2	1	0	0	−1	1	8
				$f_{12\text{-H}}(13\text{-CH}_3)$				
180	4	9	16	19	16	9	4	2
135	4	9	16	19	16	9	4	2
90	4	9	16	19	16	9	4	3
45	4	9	15	18	13	5	1	1
				$f_{14\text{-H}}(10\text{-H})$				
180	0	10	44	50	44	10	0	−1
135	−1	3	24	50	48	14	1	−1
90	0	0	2	39	41	8	1	0
45	0	0	0	9	17	3	1	1

[a] Enhancements in per cent.

deviation from planarity of the γ-torsional angle in the former. Thus, the calculations yield $\gamma \simeq -30°$ (s-cis) or $\gamma \simeq 145°$ (s-trans), while the NOE's require values in the neighborhood of $\pm 90°$. No single structure with reasonable values of γ, on the other hand, yields calculated NOE's close to the experimental values. This is true because the enhancements $f_{10\text{-H}}(13\text{-CH}_3)$ and $f_{14\text{-H}}(10\text{-H})$ are both significantly different from zero. An s-cis structure with $\beta = 170°$ and $\gamma = -29°$, which correspond to the torsional angles obtained theoretically, predicts $f_{10\text{-H}}(13\text{-CH}_3)$ to be zero; similar results are obtained when the bond angles from the theoretical structure are used. When a value of γ corresponding to a structure near the s-trans potential minimum is used ($\beta = 175°$, $\gamma = 135°$), the enhancement $f_{14\text{-H}}(10\text{-H})$ is predicted to be zero. Only by choosing a structure with $\gamma \simeq \pm 90°$, in which 10-H is sufficiently close to *both* 14-H and 13-CH_3, can one fit the NOE results.

The above dilemma can be resolved by suggesting that the 11-cis molecule in solution is an equilibrium mixture of s-cis and s-trans. If one assumes that the molecule is "jumping" between the s-cis and s-trans minima and the rate constant k for the jumping satisfies the condition $T_1^{-1} < k < \tau_c^{-1}$, which is reasonable for the barrier involved (see Figure 5),[6] the NOE's can be calculated by averaging $1/r^6$ for the two structures (Schirmer *et al.*, 1972). The resulting NOE's with equal probabilities for s-cis and s-trans structures are listed in Table VIII. For this simple average, the values are more analogous to the NOE calculations for *all-trans*-retinal; that

[6] For a barrier height of $\gtrsim 6$ kcal mol^{-1}, the rate constant k at 32° estimated using transition state theory is $\lesssim 3 \times 10^8$ sec^{-1} which is much larger than $T_1^{-1} \simeq 1$ sec^{-1} and smaller than $\tau_c^{-1} \simeq 2 \times 10^{10}$ sec^{-1}.

TABLE VIII: Calculated Nuclear Overhauser Enhancements for 11-*cis*-Retinal.

		(β,γ)					
NOE	Expt[a]	(165, 90)[b]	(165, 90)[c]	(165, −75)[b]	(165, −75)[c]	Av[b,d]	Av[c,d]
$f_{11\text{-H}}(9\text{-CH}_3)$	23	31	23	31	23	31	23
$f_{14\text{-H}}(10\text{-H})$	12	12	6	15	7	31	22
$f_{10\text{-H}}(13\text{-CH}_3)$	11	10	6	8	6	22	18
$f_{15\text{-H}}(13\text{-CH}_3)'$	30	44	31	44	31	44	31

[a] 100 MHz, 32°. [b] Including intramolecular dipole–dipole relaxation of methyl protons. [c] Including intramolecular dipole–dipole relaxation of methyl protons and other relaxation pathways (ρ_{other}) for CH protons (see text). [d] Calculated averaging $1/r^6$ for equal populations of the two structures (165,135) and (165,−45).

is, the calculated NOE's are all uniformly larger than the observed NOE's. The NOE's calculated for 11-*cis*-retinal including other relaxation pathways (ρ_{other}), where ρ_{other} is set equal in magnitude to that used to bring the all-trans calculated NOE's into agreement with the observed all-trans NOE's, are also listed in Table VIII. The result is that $f_{11\text{-H}}(9\text{-CH}_3)$ and $f_{15\text{-H}}(13\text{-CH}_3)$ are again in agreement with the observed NOE's, but $f_{14\text{-H}}(10\text{-H})$ and $f_{10\text{-H}}(13\text{-CH}_3)$ are now calculated too small for either single structure (165,90) or (165,−75) and too large from the "averaged" s-cis ↔ s-trans equilibrium. These results confirm, in agreement with the above considerations, that neither of the structures (165,90) and (165,−75) by itself represents the correct structure and that some averaging process having the essential features of that considered above is required to correctly predict the observed NOE's. However, it appears likely that the actual averaging process followed by the molecule is considerably more complicated than in the simple two-state "jumping" model assumed here. A more detailed consideration of the averaging effect on the NOE's requires an accurate knowledge of the multidimensional potential energy function and, in the classical limit, of the interconversion path. From the calculations, a likely interconversion path is to go from the s-cis minimum ($\gamma = -29°$) to $\gamma = -150°$, the β angle changing from −10 to +10° so as to reach the s-trans minimum. If this is correct and the potential has the form shown in Figure 5 with a significant barrier in the −100° region, only small contributions from a structure in the neighborhood of (165,−75) are expected. On the other hand, interconversion involving positive γ values ($\gamma \simeq -40° \rightarrow \gamma \simeq 40° \rightarrow \gamma \simeq 150°$) results in a small barrier at $\gamma \simeq 100°$ and would have significant contributions from a structure like (165,90) if the energy scale of the potential were appropriate. In this way, quantitative agreement between experimental and calculated NOE values might be achieved.

A comparison of the ambient and low-temperature NOE's (Table III) for both *all-trans*- and 11-*cis*-retinal shows that the NOE which is most changed at low temperature is $f_{14\text{-H}}(10\text{-H})$ in 11-*cis*-retinal; $f_{14\text{-H}}(10\text{-H})$ is smaller at the low temperature by an amount greater than experimental error. Balanced against the general trend of all of the NOE's of *all-trans*- and 11-*cis*-retinal to decrease slightly in going to lower temperatures, the fact that $f_{10\text{-H}}(13\text{-CH}_3)$ for 11-*cis*-retinal is unchanged at low temperature is also noteworthy; it implies that, if anything, the interaction is increased slightly. This behavior of $f_{14\text{-H}}(10\text{-H})$ and $f_{10\text{-H}}(13\text{-CH}_3)$ for 11-*cis*-retinal as a func-

tion of temperature is consistent with the partial freezing out of the s-trans conformer. The effect can be quantitatively duplicated in the calculated NOE's by increasing the fractional population of the s-trans conformer in the simple two-state jumping model considered above. This result indicates that it is the s-trans conformer which is, in fact, the more stable in acetone-d_6. However, the required potential energy difference between the two conformations is so small (<1 kcal mol^{-1}) that solvent effects might well be involved in the observed equilibrium.

The chemical-shift changes upon going to low temperature are shown in Table II to be approximately the same for most of the protons of *all-trans*- and 11-*cis*-retinal. The largest exceptions are 13-CH_3, 8-H, and 10-H which are shifted *more* downfield at low temperature in 11-cis than all-trans by 0.059, 0.061, and 0.092 ppm, respectively. The changes in 13-CH_3 and 10-H are consistent with the above suggestion that the relative contribution of the two forms, s-cis and s-trans, is significantly changed at low temperature.

Conclusion

The above studies have shown that the polyene chain of *all-trans*-retinal has a planar conformation with all of the single bonds from C-7 to C-15 in the s-trans conformation. 11-*cis*-Retinal is shown to be essentially planar in the regions C-7–C-10 and C-13–C-15, but exists as an equilibrium between two low-energy conformers, distorted s-cis and distorted s-trans, about the 12–13 single bond. The distorted s-trans conformer appears to be preferred at low temperatures in acetone solution. An important conclusion which follows from the experimental and theoretical work reported here is that the two conformations (12-s-cis and 12-s-trans) of 11-*cis*-retinal are very similar in energy (within 1 kcal/mol). This suggests that when bound to the protein opsin to form rhodopsin, retinal could have either conformation about the 12–13 bond; in fact, given reasonable constraints supplied by the opsin, a wide range of dihedral angles is expected to be accessible to 11-*cis*-retinal. Within ~2 kcal/mole, significant twists about other nominal single bonds (*e.g.*, 8–9) as well as smaller distortions of the nominal double bonds are possible. Such effects could play an important role in the spectroscopic and functional properties of the chromophore retinal as part of rhodopsin. It also raises the possibility that the photochemical process involves simultaneous isomerization about the 11–12 double bond and one of the single bonds so as to keep fixed the position of certain groups of the retinal bonded to the protein (*e.g.*, the carbonyl as a Schiff's base) or in contact with it (*e.g.*, the cyclohexene ring).

Acknowledgments

The authors would like to thank Paul Brown for generous gifts of 11-*cis*-retinal and helpful discussions, Dr. Bruce Hudson for assistance during the initial stages of these experiments, Drs. J. Dadok and R. Sprecher for assistance in obtaining 250-MHz spectra, Mme. Giessner-Prettre for providing the torsional angles from the crystal structure of *all-trans*-retinal, S. L. Patt for helpful discussions and instrument modifications, and W. E. Hull and M. Granville for assistance with programming.

References

ApSimon, J. W., Craig, W. G., Demarco, P. V., Mathieson, D. W., Saunders, L., and Whalley, W. B. (1967a), *Tetrahedron 23*, 2339.

ApSimon, J. W., Craig, W. G., Demarco, P. V., Mathieson, D. W., Saunders, L., and Whalley, W. B. (1967b), *Tetrahedron 23*, 2351.

ApSimon, J. W., Demarco, P. V., Mathieson, D. W., Craig, W. G., Karim, A., Saunders, L., and Whalley, W. B. (1970), *Tetrahedron 26*, 119.

Barfield, M. (1971), *J. Amer. Chem. Soc. 93*, 1066.

Barfield, M., and Chakrabarti, B. (1969), *Chem. Rev. 69*, 757.

Bothner-By, A. A., and Castellano, S. (1964), *J. Chem. Phys. 41*, 3863.

Bothner-By, A. A., and Jung, D. (1968), *J. Amer. Chem. Soc. 90*, 2342.

Cooper, M. A., Elleman, D. D., Pearce, D. C., and Manatt, S. L. (1970), *J. Chem. Phys. 53*, 2343.

Dadok, J., Sprecher, R. F., Bothner-By, A. A., and Link, T. (1970), 11th Experimental NMR Conference, Pittsburgh, Pa.

Douglas, A. W., and Goldstein, J. H. (1965), *J. Mol. Spectrosc. 16*, 1.

Freeman, R., Wittekoek, S., and Ernst, R. R. (1970), *J. Chem. Phys. 52*, 1529.

Gilardi, R., Karle, I. L., Karle, J., and Sperling, W. (1971), *Nature (London) 232*, 187.

Gilardi, R. D., Karle, I. L., and Karle, J. (1972), *Acta Crystallogr., Sect. B 28*, 2605.

Hamanaka, T., Mitsui, T., Ashida, T., and Kakudo, M. (1972), *Acta Crystallogr., Sect. B 28*, 214.

Hobgood, R. T., and Goldstein, J. H. (1964), *J. Mol. Spectrosc. 12*, 76.

Holmes, J. R., and Kivelson, D. (1961), *J. Amer. Chem. Soc. 83*, 2959.

Honig, E., Hudson, B., Sykes, B. D., and Karplus, M. (1971), *Proc. Nat. Acad. Sci. U. S. 68*, 1289.

Honig, B., and Karplus, M. (1971), *Nature (London) 229*, 558.

Johnson, L. (1965), Varian Associates Technical Information Bulletin, Palo Alto, Calif., Varian Associates, Summer, p 7.

Karplus, M. (1959), *J. Chem. Phys. 30*, 11.

Karplus, M. (1960), *J. Chem. Phys. 33*, 1842.

Karplus, M. (1969), *J. Chem. Phys. 50*, 3134.

Klyne, W., and Prelog, V. (1960), *Experientia 16*, 521.

Kuhlman, K. F., Grant, D. M., and Harris, R. K. (1970), *J. Chem. Phys. 52*, 3439.

Langlet, J., and Giessner-Prettre, G. (1972), *J. Mol. Struct. 13*, 317.

Langlet, J., Pullman, B., and Berthod, H. (1970), *J. Mol. Struct. 6*, 139.

Montaudo, G., Librando, V., Caccamese, S., and Marauigna, P. (1973), *J. Amer. Chem. Soc. 95*, 6365.

Nash, H. A. (1969), *J. Theor. Biol. 22*, 314.

Noggle, J. H., and Shirmer, R. E. (1971), The Nuclear Overhauser Effect, New York, N. Y., Academic Press, p 115.

Patel, D. (1969), *Nature (London) 221*, 825.

Patel, D., and Shulman, R. G. (1970), *Proc. Nat. Acad. Sci. U. S. 65*, 31.

Pullman, B., Langlet, J., and Berthod, H. (1969), *J. Theor. Biol. 23*, 482.

Schirmer, R. E., Davis, J. P., Noggle, J. H., and Hart, P. A. (1972), *J. Amer. Chem. Soc. 94*, 2561.

Schirmer, R. E., Noggle, J. H., Davis, J. P., and Hart, P. A. (1970), *J. Amer. Chem. Soc. 92*, 3266.

Segre, A. L., and Castellano, S. (1972), *J. Magn. Resonance 7*, 5.

Sutton, L. E. (1965), *Chem. Soc., Spec. Publ. No. 18*, S-15.

Traetteberg, M. (1970), *Acta Chem. Scand. 24*, 373.

Vold, R. L., Waugh, J. S., Klein, M. P., and Phelps, D. E. (1968), *J. Chem. Phys. 48*, 3831.
Wald, G. S. (1968), *Science 162*, 230.
Warshel, A., and Karplus, M. (1972), *J. Amer. Chem. Soc. 94*, 5612.
Wennerström, H. (1972), *Mol. Phys. 24*, 69.

Circular Dichroism Studies of the Conformational Stability of Dinucleoside Phosphates and Related Compounds in Aqueous Neutral Salt Solutions†

Neil P. Johnson and Thomas Schleich*

ABSTRACT: Circular dichroism spectra were recorded for adenylyl-(3′–5′)-adenosine, adenylyl-(3′–5′)-uridine, uridylyl-(3′–5′)-adenosine, adenosine 5′-mononicotinate, and uridylyl-(3′–5′)-adenosine phosphonate in a variety of neutral salt solutions and several organic solvents as a function of temperature and pH. The additives altered the circular dichroism spectra of dinucleoside phosphates and adenosine 5′-mononicotinate as a consequence of induced conformational changes. Uridylyl-(3′–5′)-adenosine phosphonate, however, displayed no optical activity attributable to base–base interactions, even at low temperature and in the presence of stabilizing salts. Perturbation of electronic transitions by solvent additives was ruled out as a major contribution to spectral changes. Most neutral salts, dioxane, and methanol unstacked the dinucleoside phosphates and the observed sensitivities to additives resembled those recorded for DNA. In contrast to the naturally occurring dinucleotides, the degree of stacking in adenosine 5′-mononicotinate was enhanced by inorganic electrolytes while nonpolar additives (such as long-chained tetraalkylammonium salts) disrupted the stacked state; these results suggest that polar and nonpolar additives which alter dinucleotide conformation according to the Hofmeister series act by different mechanisms. The absence of detectable stacking in uridylyl-(3′–5′)-adenosine phosphonate demonstrates the importance of phosphodiester backbone stereochemistry to the maintenance of the stacked state. Both ΔH and ΔS (for unstacked → stacked) were negative and decreased in absolute magnitude in the presence of denaturing agents; stabilizing salts had the opposite effect. Lowering the pH unstacked adenylyl-(3′–5′)-adenosine, adenosine 5′-mononicotinate, and adenylyl-(3′–5′)-uridine. The conformation of uridylyl-(3′–5′)-adenosine, however, did not change over the observed pH range. The results of this study illustrate the contributions of both solvophobic bonding interactions and phosphodiester backbone stereochemistry to the conformational form and stability of dinucleoside phosphates in solution.

Base-stacking interactions are generally thought to provide a major contribution to the overall energetics defining polynucleotide conformation in solution (for a recent review, see Cantor and Katz, 1971). These interactions are characterized as solvophobic (enthalpy driven–entropy opposed) (Lowe and Schellman, 1972) in contradistinction to the Kauzmann hydrophobic bond (entropy driven–enthalpy opposed) which is considered responsible for the association of hydrocarbon moieties in aqueous solution. Recently, conformational energy calculations have also shown the importance of phosphodiester backbone stereochemistry in defining the conformational form of polynucleotides (Olson and Flory, 1972a–c; Govil, 1973; Perahia *et al.*, 1973; Sasisekharan, 1973).

Physical biochemists interested in questions of nucleic acid conformational stability have studied the constituents of polynucleotides in order to separate the contributions of solvophobic bonding from the effects of electrostatic backbone interactions, hydrogen bonding, and cooperativity. Typical examples include studies of monomer base association (for a review, see Ts'o, 1970, Scruggs *et al.*, 1972, and Herskovits and Harrington, 1972), studies of nucleoside and nucleotide conformation by nmr[1] and CD (Prestegard and Chan, 1969; Formoso, 1972; Schleich *et al.*, 1972) and studies of dinucleoside phosphate conformation utilizing nmr and optical spectroscopy (Leng and Felsenfeld, 1966; Brahms *et al.*, 1967; Davis, 1967; Davis and Tinoco, 1968; Chan and Nelson, 1969; Kondo *et al.*, 1970; Lowe and Schellman, 1972; Ts'o *et al.*, 1969; Smith *et al.*, 1973).

We undertook the present circular dichroism experiments to investigate the conformational form and stability of dinucleoside phosphates in solution. We were also interested in obtaining additional information about the mechanism(s) of the Hofmeister effect. Neutral salts, organic solvents, low pH, and temperature were used as conformational perturbants. Model compounds were chosen which might be expected to reveal the contributions of solvophobic interactions and backbone stereochemistry to dinucleotide conformation.

ApA[1] was chosen because it is the most widely studied di-

† From the Division of Natural Sciences, University of California, Santa Cruz, California 95064. *Received August 14, 1973.* This work was supported by a grant from the National Science Foundation (GB 19503).

[1] Abbreviations used are: ApA, adenylyl-(3′–5′)-adenosine; ApU, adenylyl-(3′–5′)-uridine; UpA, uridylyl-(3′–5′)-adenosine; AMN, adenosine 5′-mononicotinate; UpcA, uridylyl-(3′–5′)-adenosine phosphonate; AMP, adenosine 5′-monophosphate; A, adenosine; U, uridine; TMACl, tetramethylammonium chloride; TEACl, tetraethylammonium chloride; TPACl, tetrapropylammonium chloride; GdmCl, guanidinium hydrochloride; $T_{1/2}$, temperature at the midpoint of a thermally induced transition; CD, circular dichroism; nmr, nuclear magnetic resonance.